QRB Discovery

www.cambridge.org/qrd

The potential of fluorogenicity for single molecule FRET and DyeCycling

Srijayee Ghosh and Sonja Schmid

Department of Chemistry, University of Basel, Basel, Switzerland

Perspective

Cite this article: Ghosh S, Schmid S (2024). The potential of fluorogenicity for single molecule FRET and DyeCycling. *QRB Discovery*, **5**: e8, 1–9 https://doi.org/10.1017/qrd.2024.11.

Received: 08 July 2024
Revised: 09 September 2024
Accepted: 11 September 2024

Keywords:
fluorescence; FRET; fluorogenic; conformational dynamics; single molecule kinetics

Corresponding author:
Sonja Schmid;
Email: sonja.schmid@unibas.ch

Abstract

Single Molecule Förster Resonance Energy Transfer (smFRET) is a popular technique to directly observe biomolecular dynamics in real time, offering unique mechanistic insight into proteins, ribozymes, and so forth. However, inevitable photobleaching of the fluorophores puts a stringent limit on the total time a surface-tethered molecule can be monitored, fundamentally limiting the information gain through conventional smFRET measurements. DyeCycling addresses this problem by using reversibly – instead of covalently – coupled FRET fluorophores, through which it can break the photobleaching limit and theoretically provide unlimited observation time. In this perspective paper, we discuss the potential of various fluorogenic strategies to suppress the background fluorescence caused by unbound, freely diffusing fluorophores inherent to the DyeCycling approach. In comparison to nanophotonic background suppression using zero-mode waveguides, the fluorogenic approach would enable DyeCycling experiments on regular glass slides with fluorogenic FRET probes that are quenched in solution and only fluoresce upon target binding. We review a number of fluorogenic approaches and conclude, among other things, that short-range quenching appears promising for realising fluorogenic DyeCycling on regular glass slides. We anticipate that our discussion will be relevant for all single-molecule fluorescence techniques that use reversible fluorophore binding.

Introduction

Fluorogenicity is the ability to transform the state of a fluorophore from a 'dark' to a 'bright' state, usually caused by a trigger event, such as target binding or a laser pulse, which changes the fluorophore structure and/or its local environment (Figure 1). A critical number is the fluorogenic ratio, i.e., the ratio of the fluorescence of the high-emission to low-emission forms, which can reach up to four orders of magnitude (Kozma and Kele, 2019). In a range of sensing and imaging works, fluorogenicity has been a valuable tool to enhance measurement contrast by suppressing non-specific fluorescence background and the noise resulting from it. For example, Liu et al. detect drug-induced proteome stress using a protein aggregation-specific fluorogenic probe, an improvement over prior cytotoxic assays (Liu *et al.*, 2017). Aggregation Induced emission (AIE) has been used to screen the effectiveness of antibiotics against bacterial growth, laying the foundation for personalized medicine (Zhao *et al.*, 2015). Molecular beacons (MBs) have been widely used since their introduction in 1996 (Tyagi and Kramer, 1996), for example in monitoring PCR (Wang and Yang, 2013), as pathogen diagnostic tools (Abravaya *et al.*, 2003), and recently in super-resolution microscopy via DNA-PAINT (Kim and Li, 2023). Fluorogenic RNA aptamers allow for precise detection and quantification of RNA production (Lu *et al.*, 2023). In microscopy applications, fluorogenicity allows the observation of target-bound probes over freely diffusing ones at high contrast, thus enabling wash-free imaging (Werther *et al.*, 2021).

Single-molecule Förster resonance energy transfer (smFRET) is used widely for studying biomolecular dynamics in the range of 2–8 nm (Ha *et al.*, 2024). In its conventional implementation, a donor and acceptor fluorophore pair is site-specifically coupled to the biomolecule of interest. The energy transfer efficiency (E) from the donor to the acceptor results from the interaction of the donor and acceptor transition dipoles and scales with the inter-fluorophore distance (R) as $E = (1 + (R/R_0)^6)^{-1}$, where the pair-specific constant R_0 is the Förster radius at which $E = 0.5$. Experimentally, E can be obtained from the individual donor and acceptor fluorescence intensities as $E = I_A/(I_D + I_A)$, subject to experiment-specific corrections (Hellenkamp *et al.*, 2018). Thanks to its strong nanoscale distance dependence, smFRET is sometimes called 'a molecular ruler'. Indeed, it can reveal conformational changes of biomolecules in real-time, providing spatio-temporal information that is missed by structural biology techniques like cryo-electron microscopy or X-ray diffraction. Moreover, owing to its single-molecule resolution, smFRET is capable of resolving steady-state dynamics in- and out-of-equilibrium as well as static sample heterogeneity (Lerner *et al.*, 2021). In the experiment, single-molecule resolution is achieved with microscope designs that minimize background fluorescence and associated noise by exciting only a small sample volume, which is realised most commonly using confocal or total internal reflection (TIR) fluorescence microscopes

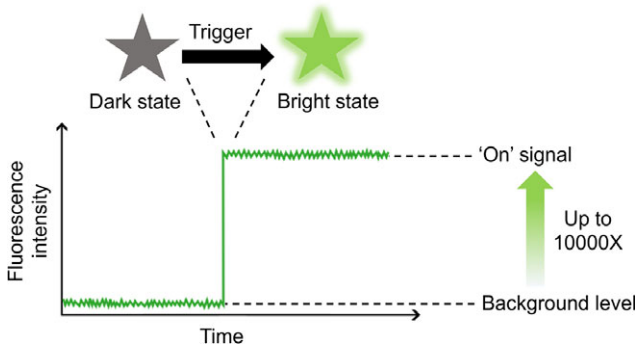

Figure 1. Schematic fluorogenic behaviour: a trigger event transforms the fluorophore from a dark to a brightly-emitting state. Fluorogenic ratios (bright to dark) of 10,000:1 can be achieved (Kozma and Kele, 2019).

(Ha *et al.*, 2024). To monitor functional dynamics of a given protein over seconds or minutes, the biomolecule of interest is often tethered to a passivated surface, where hundreds to thousands of single molecules can be recorded in parallel using wide field detection by s-CMOS or EM-CCD cameras in TIR microscopes. Over the past three decades, smFRET has rapidly evolved from a niche technique to a widely popular approach to answering fundamental questions in biology (Ha *et al.*, 2024).

Still, surface-tethered smFRET experiments are fundamentally limited by irreversible photobleaching of the covalently labelled fluorophores (Figure 2A). Each organic fluorophore molecule, used as FRET donor or acceptor, has a finite photon budget before its photoinduced degradation or photobleaching (Zheng and Lavis, 2017). This fact forces the experimenter to choose between obtaining a high signal-to-noise ratio (SNR) with a high excitation laser power leading to faster bleaching or a longer observation time with a low laser power and thus low SNR. Currently, the achieved temporal bandwidth in smFRET literature (spanning from the shortest to the longest measurable time interval) spans only 2–3 orders of magnitude in time (Vermeer and Schmid, 2022). Despite efforts in developing more photostable self-healing fluorophores (Altman et al., 2012; Isselstein et al., 2020; Pati et al., 2020; Zheng et al., 2014) and the development of photostabilizers, such as oxygen scavengers (Benesch and Benesch, 1953; Aitken et al., 2008; Swoboda et al., 2012) and triplet state quenchers (Rasnik *et al.*, 2006; Roy *et al.*, 2008; Vogelsang *et al.*, 2008), eventual photobleaching leads to an unwanted, early end of the smFRET experiment. Several biomolecular processes occur on timescales beyond the current observation limit of 2–3 orders of magnitude in time (Vermeer and Schmid, 2022). For example, the bacterial RNA polymerase makes processing pauses of tens to hundreds of seconds (Janissen *et al.*, 2022) before continuing RNA polymerization, which are timescales that are out of reach for conventional smFRET experiments with reasonable time resolution of milliseconds. Also, ribosomal translation observed in smFRET experiments (with one covalent donor and multiple acceptors in a row) was limited to the detection of only 12 amino acid transfers (Tsai *et al.*, 2016), while the median human protein consists of 375 amino acids (Brocchieri and Karlin, 2005), converting to >1 h translation time in such room temperature experiments. As a result, co-translational effects and many other biological processes remain far beyond the accessible timescales of today's smFRET experiments. In particular, rare but decisive events, such as bursting and pausing, are hard or impossible to study by conventional smFRET and may even be discarded as 'odd' outlier events, while magnetic tweezers (Janissen *et al.*, 2022), nanopores (Nova *et al.*, 2024), and fluorescent product detection (English *et al.*, 2006) demonstrate their prevalence in protein function. Also, the observations of long-lived dynamic disorder and large fluctuations in enzyme catalytic rates (van Oijen *et al.*, 2003) emphasize the importance of a per-molecule analysis that DyeCycling aims to provide.

Moreover, current analysis approaches that combine data of many molecules to extract global kinetic models (the best option currently, some are listed in Table 1 in Lerner et al., 2021) rely on the ergodic assumption, while Thirumalai and co-workers showed effective ergodicity breaking already for simple DNA-based Holliday junctions (Hyeon *et al.*, 2012). Their findings hint at even more such complexity in protein systems. Hence, pooling many single-molecule traces together for a global analysis remains a non-ideal workaround, as long as the ergodic assumption is not verified for the studied dataset. Lastly, also from an energy perspective, the currently achieved temporal bandwidth of smFRET (2–3 orders of magnitude in time) is suboptimal. This bandwidth limits the maximum equilibrium constant (K) and hence Gibbs free energy that can be probed with conventional smFRET. For example, it translates to approximately 1/3–1/2 of the energy provided by ATP hydrolysis (ca. 30 kJ/mol depending on buffer conditions) (Rosing and Slater, 1971), as obtained by $dG = -RT\ln(K)$ with $T = 300$ K, equilibrium constant $K = k_1/k_2 = 100$ to 1000 , where k_1 and k_2 are the fastest and slowest measurable processes within the bandwidth, respectively. Notably, this general thermodynamic statement holds for conventional smFRET experiments with various time resolutions.

DyeCycling can overcome these issues (Figure 2B): using reversible binding and dissociation of the fluorophores (or "dyes"), it decouples the observation of a given biomolecule from the photobleaching of just one fluorophore (Vermeer and Schmid, 2022) – a trick that has previously revolutionized super-resolution imaging through Point Accumulation for Imaging in Nanoscale Topography (PAINT) (Sharonov and Hochstrasser, 2006; Jungmann et al., 2010). DyeCycling, however, is not an imaging technique: instead of images with high resolution in space, DyeCycling resolves (bio-)molecular dynamics in time. More precisely, it broadens the temporal bandwidth of smFRET experiments, such that previously inaccessible biomolecular processes can be studied, e.g., the fast processing of RNA-polymerase interspaced by long pausing (Janissen *et al.*, 2022). While the concept of DyeCycling was initially demonstrated using reversible DNA hybridization of fluorescently labelled cycler oligos to ssDNA docking strands coupled to the biomolecule of interest (similar to Renewable Emission via Fluorogenic and Repeated ssDNA Hybridisation, REFRESH-FRET (Kümmerlin *et al.*, 2023)), technically every reversible coupling chemistry with suitable binding kinetics can be used. Two points are thereby key for the DyeCycling experiment: First, relatively high concentrations (ca. 1 μM) of free-floating fluorescent cyclers are needed for fast binding rates (ca. 1/s), in order to achieve nearly 100% cycler-pair-bound coverage and minimize unbound 'blind gaps'. Second, as a result, good background suppression is crucial to keep the noise level low and achieve smFRET trajectories with good SNR. The upper limit of tolerable fluorophore concentrations in solution for typical TIR setups is ≤100 nM. Zero-mode waveguides (ZMWs) present a viable *physical* solution (Levene *et al.*, 2002; Crouch *et al.*, 2018) for background suppression in DyeCycling experiments, as will be published elsewhere. This is because they offer particularly small excitation volumes in the zeptoliter range

https://doi.org/10.1017/qrd.2024.11 Published online by Cambridge University Press

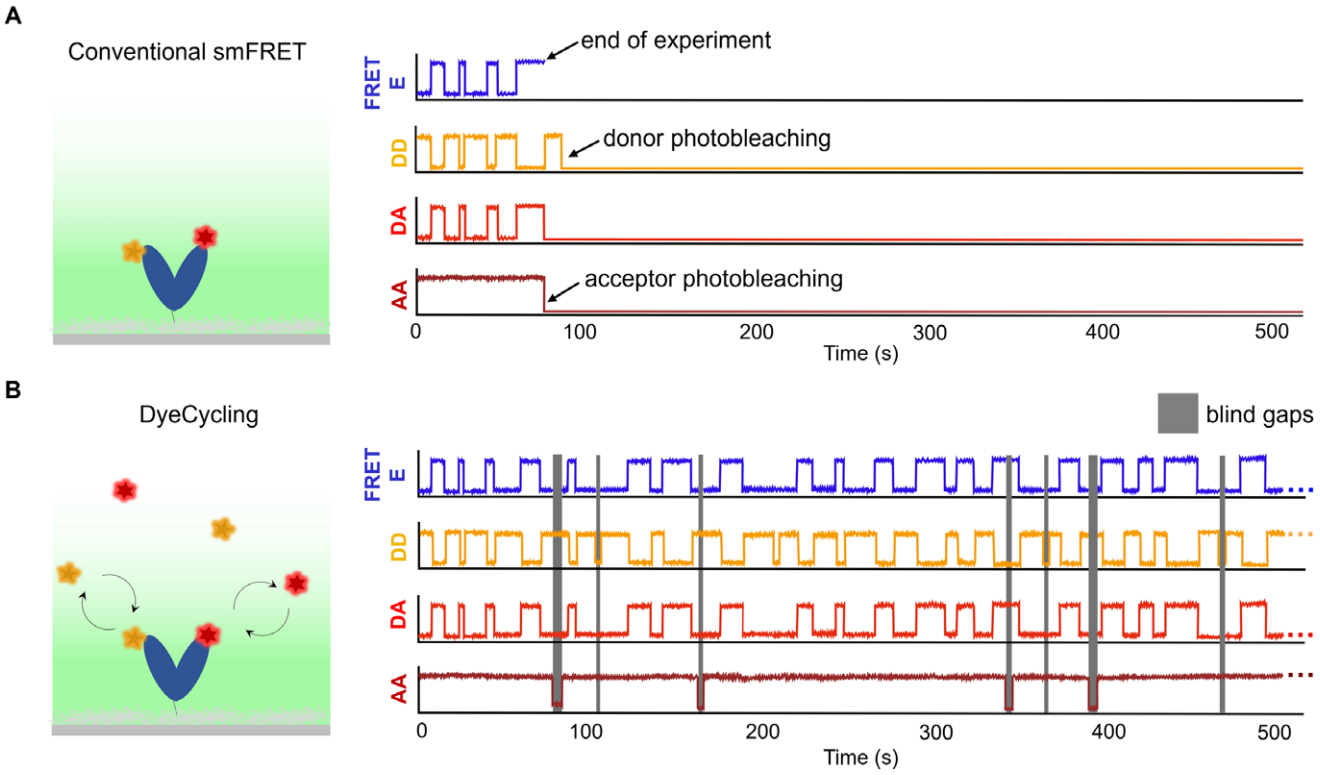

Figure 2. Conventional smFRET vs DyeCycling. (A) Conventional smFRET illustrated with the covalently attached donor (yellow) and acceptor (red) fluorophores bound to the biomolecule under study. Schematic FRET time traces (blue) illustrate the short observation time of conventional smFRET due to irreversible photobleaching of the donor or the acceptor fluorophore. DA: FRET-sensitized acceptor emission after donor excitation; DD: donor emission after donor excitation; AA: acceptor emission after acceptor excitation; (B) Cartoon of DyeCycling with reversibly binding donor and acceptor fluorophores in solution. The schematic time traces illustrate that DyeCycling is not limited by photobleaching of individual fluorophores and can theoretically continue for hours. The grey shaded areas represent pauses with incomplete FRET pairs (donor and/or acceptor missing). The typical sampling rate of 100 ms is assumed here.

(Yang *et al.*, 2023). However, ZMWs require nanofabrication know-how and equipment, while reliable commercial solutions are costly or even lacking.

Here, we explore fluorogenicity as an alternative *chemical* solution for background suppression in DyeCycling experiments (Figure 3A). Since fluorogenic cyclers would only become bright upon specific target binding, causing minimal background fluorescence when unbound, fluorogenic DyeCycling would facilitate high-quality smFRET recordings using common, cheap microscopy slides or coverslips. In this perspective paper, we discuss various fluorogenic systems (Figure 3B) with a focus on their potential for DyeCycling-based smFRET experiments, the requirements of which are summarized in Box 1. More general fluorogenicity reviews covering more physico-chemical mechanisms exist already elsewhere (Kozma and Kele, 2019; Li *et al.*, 2017b; Lu *et al.*, 2023).

Box 1: Requirements for fluorogenic DyeCycling probes

- ✓ **A strong fluorogenic ratio** of ≥10 is desired to efficiently suppress the background fluorescence and noise of unbound cyclers in solution (Kozma and Kele, 2019).
- ✓ **Optimal photophysics:** high photostability, minimal blinking, ideally a high extinction coefficient $\varepsilon > 50{,}000\ M^{-1}\ cm^{-1}$ (Ha *et al.*, 2024) and ideally a quantum yield QY > 0.6, and minimal cross-talk between donor and acceptor fluorophores are important criteria for fluorogenic systems compliant with DyeCycling.
- ✓ **FRET characteristics** include further a sufficiently large overlap integral between donor emission and acceptor excitation spectra and no interference of the fluorogenic systems of the donor and acceptor with FRET.
- ✓ **Small size and short linkers:** precise inter-fluorophore distance determination by smFRET ideally requires small point probes with short linkers (i.e., small fluorophore-accessible volumes), yet ample orientational freedom. Large probes can sterically affect biomolecular dynamics, hence, small organic probes (~1 nm) are generally preferred.
- ✓ **Water-solubility** of the fluorogenic probe is required for DyeCycling in aqueous buffers. Coupling auxiliary hydrophilic groups (even DNA) to the fluorogenic species can improve solubility.
- ✓ **Suitable binding kinetics:** dissociation rates faster than the bleach rate and ideally diffusion-limited binding rates enable minimal blind gaps and maximal observation time in DyeCycling experiments.
- ✓ **Site-specific binding** of the donor as well as the acceptor probe to the biomolecule of interest at the desired position is necessary and can be achieved through a range of bioconjugate techniques.

Altogether, the requirements for fluorogenic DyeCycling are more stringent than for (super-resolution) imaging applications.

Fluorogenic mechanisms and their applications

Removal of a quencher

Fluorophore-quencher pairs are popular fluorogenic systems, where the fluorophore is dark when a quencher molecule is nearby, and the fluorescence is restored by removal of this quencher. Quenching can occur via several distance-dependent mechanisms (Crisalli and Kool, 2011): through energy transfer (similar to FRET) if the quencher is within 2–10 nm of the fluorophore, or through shorter-range quenching if they are <2 nm apart. These short-range

https://doi.org/10.1017/qrd.2024.11 Published online by Cambridge University Press

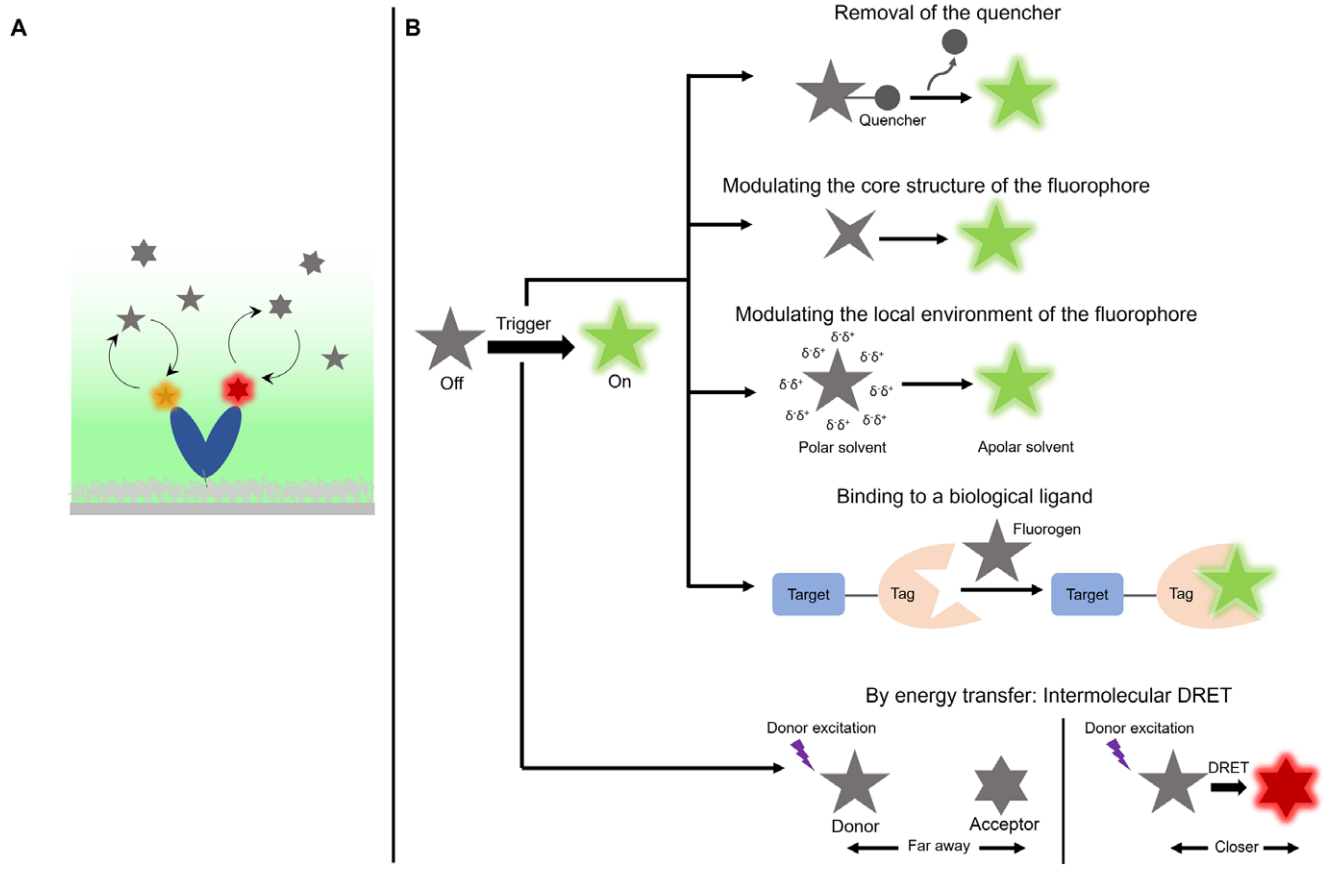

Figure 3. (A) Schematic representation of fluorogenic DyeCycling, where the donor and acceptor fluorophores are dark in solution but become fluorescent upon binding to the molecule of interest. Donor and acceptor are continuously replaced with the respective fluorophores in solution. (B) Several fluorogenic mechanisms exist to turn a dark fluorogen into a brightly fluorescent one. We categorize them into: removal of a quencher, modulation of the fluorogen's core structure, modulation of its local environment, or binding to a biological ligand. Alternatively, apparent fluorogenicity results from energy transfer to another bright molecule.

mechanisms include static contact quenching (e.g., by π–π stacking), dynamic collisional quenching in the excited state, photoinduced electron transfer (PET) driven by redox chemistry, and Dexter electron transfer via spectral overlap between the electron donor and acceptor (Goldberg *et al.*, 2013).

A molecular beacon (MB) is a single-stranded DNA (ssDNA) probe with a fluorophore and a quencher at its two ends, which forms a hairpin structure causing close end-to-end proximity and thus fluorescence quenching. Binding to a complementary ssDNA target disrupts the hairpin, thereby separating quencher and fluorophore in space, which de-quenches the fluorescence. For super-resolution (PAINT) imaging, an MB-PAINT was designed with a target sequence (9 nt) partially embedded in the stem and partially exposed in the loop (Figure 4A) to accelerate target binding over conventional MB (Kim and Li, 2023). Nevertheless, MB-PAINT binding remained ca. 70-fold slower compared to unhindered hybridization, due to the competition with the intramolecular hairpin – a disadvantage for potential use in DyeCycling. Alternatively, longer (15 nt) ssDNA with fluorophore and quencher (Cy3B/BHQ2 and ATTO 643/IBFQ) at opposite ends were used for fluorogenic DNA-PAINT where mismatches were introduced to facilitate reversible binding (Chung *et al.*, 2022). This approach was also used in REFRESH-FRET (Kümmerlin *et al.*, 2023), using the fluorophore-quencher pair Cy3B-BHQ2 or using contact quenching of two ATTO 647N molecules. While the latter tolerates shorter ssDNA strands (i.e., favourable faster dissociation), the two bright ATTO 647N molecules, once de-quenched, complicate the smFRET readout (increased noise, Homo-FRET, etc.).

In general, for energy transfer-based quenchers, the fluorophore-quencher separation required for efficient dequenching (ca. 2^*R_0 with R_0 = 3.5–7.5 nm (Le Reste *et al.*, 2012)) imposes a lower limit for the duplex length (7–15 nm or 21–45 nt), and thus an upper limit for the dissociation rate, which can only be increased to some extent by base-pair mismatches. Hence, short-range quenching mechanisms appear promising in this regard: e.g., contact quenching using dinitroaniline, trinitroaniline, or carbazole (Sunbul and Jäschke, 2013), or photo-induced electron transfer to tryptophan or guanine (Doose *et al.*, 2009).

Tetrazine groups – well-known from bio-orthogonal click chemistry (Deng *et al.*, 2024) – were elegantly used as quenchers in fluorogenic probes. Here tetrazine-coupled fluorophores de-quench upon reaction with a strained alkene substrate such as trans-cyclooct-2-ene (TCO) via the irreversible Inverse Electron Demand Diels – Alder (IEDDA) reaction, causing strong fluorogenicity (up to 39-fold (Beliu *et al.*, 2019)). Quenching by tetrazine may involve resonant energy transfer (in case of spectral overlap of fluorophore emission and tetrazine absorption, ca. 520–540 nm (Pinto-Pacheco *et al.*, 2020), PET from the excited fluorophore to the tetrazine (Beliu *et al.*, 2019), as well as through-bond energy transfer (TBET, i.e., energy transfer from the fluorophore to tetrazine via a conjugated linker). Based on the latter, Loredo et al. developed a class of TBET-based photo-activatable probes for

https://doi.org/10.1017/qrd.2024.11 Published online by Cambridge University Press

super-resolution imaging, based on coumarin, rhodamine, and BODIPY. In these systems, tetrazine undergoes photolysis, releasing nitriles and molecular nitrogen, yielding up to a 178-fold increase in BODIPY fluorescence, however only after 20 min of irradiation at 254 nm with 1400 μWcm^{-2} (Loredo *et al.*, 2020). Beyond the long photo-activation time and potentially damaging UV radiation, the irreversible bond formed is unsuitable for use in DyeCycling. The challenge would lie in making this strong fluorogenic probe a reversible binder that responds to longer-wavelength radiation.

Changes in the core structure of the fluorophore

The emission of an organic fluorophore can be modulated by changing its conjugated system (sometimes called its "core"), e.g., by a chemical reaction upon target binding or by a light pulse. The dynamic equilibrium of rhodamines between a non-fluorescent spirocyclic form and a fluorescent zwitterionic form was harnessed to create fluorogenic Silicon Rhodamines (SiRs). The equilibrium shifts to the fluorescent, zwitterionic form upon binding to the target, a HaloTag in this case (Si *et al.*, 2023). Interestingly, besides the well-known covalent HaloTag ligands, Kompa et al. developed a series of exchangeable ligands that enable non-covalent, reversible labelling of the HaloTag ($K_D \cong 10^{-8}$ M) with a fluorogenic ratio of 10 (Figure 4B; Kompa *et al.*, 2023). Also, fluorogenic SNAP-tag ligands were developed by exploiting the intramolecular cyclization of derivatives of commonly used cyanines (Cy3, Cy5, Cy7) conjugated with nucleophilic side chains. While a good fluorogenic ratio of up to 124 was achieved (Martin and Rivera-Fuentes, 2024), we are unaware of reversible SNAP-tag ligands of this kind, which precludes their application in DyeCycling. Altogether, while initially developed for imaging applications, reversible self-labelling is potentially interesting for DyeCycling, too. However, the large size of the current protein tags (HaloTag7: 34 kDa, SNAP-tag: 19.4 kDa) would significantly compromise site-specific positioning as well as the sub-nanometer resolution of smFRET (Ha et al., 2024; Sustarsic and Kapanidis, 2015).

Light-induced fluorogenicity occurs in photoactivatable fluorophores, whose core structure can be photochemically converted from a non- or weakly emissive state into a bright emissive state. Typical implementations involve a caging group (e.g., 2-nitrobenzyl derivatives) that is removed by UV irradiation (Banala *et al.*, 2012). Reversible photoactivation was further realized using rhodamine spiroamides that exist in a non-fluorescent 'closed' isomer and a highly emissive 'open' xanthylium isomer (λ_{em} ~580 nm). UV absorption (366 nm) by the closed isomer triggers conversion to the fluorescent open isomer via conjugation in the xanthene ring. The open isomer has a lifetime of 20–100 ms in polar solvents (Fölling *et al.*, 2007), until thermal conversion to the dark isomer or photobleaching takes place. Besides this very short bright life time, their utility is further limited by aggregation, non-specific adhesion, and low water solubility. Additionally, prompted by concerns about UV-induced damage to biomolecules, efforts were made to shift the photoswitching to a visible-range wavelength of 405 nm (Lee *et al.*, 2014). However, for DyeCycling, light-induced dissociation from the target molecule would be more useful than light-induced activation of all fluorophores in solution, causing unwanted background fluorescence.

Changes in the local environment of the fluorophore

Aggregation-caused quenching (ACQ) occurs through contact quenching, when certain fluorophores come into close proximity, causing strong π–π interactions through which the excited state decays via non-radiative photophysical pathways (Zhao and Chen, 2021). ACQ can arise due to the hydrophobic interactions in polar solvents, such as water, while the aggregates disassemble in apolar environments, generating a fluorogenic response. Intercalating fluorophores, such as amyloid-binding Thioflavin T (Hanczyc *et al.*, 2021) and DNA-binding YOYO-1, work in similar ways: e.g., the dimeric YOYO-1 is non-fluorescent in water but opens upon DNA intercalation (Klymchenko, 2017), causing an over 1000-fold fluorescence increase. Conversely, aggregation-induced emission (AIE) refers to the opposite effect, where a fluorophore, quenched in solution, shows fluorescence enhancement upon aggregation. In this case, non-radiative relaxation in solution can occur through rotational and vibrational motions that get hindered upon aggregation, thus giving rise to aggregation-induced fluorogenic behaviour. For example, the tetraphenylethene is non-emissive when dissolved but becomes emissive upon aggregation, which limits the rotational freedom of its phenyl rotors and diphenylmethylene units. Such AIEgens are used in biosensing and fluorescence microscopy, where they were found to be superior to conventional organic fluorophores and quantum dots (Mei *et al.*, 2015). However, the multiple closely-spaced fluorophores in ACQ and AIE are incompatible with precise single-molecule readouts, including smFRET and DyeCycling.

Binding to a protein or aptamer

Fluorogen-activating proteins (FAPs) are genetically encoded protein tags that bind specific fluorogens non-covalently, which stabilizes the emissive conformation of the fluorogen (e.g., thiazole orange, malachite green) (Li *et al.*, 2017b). The resulting bright fluorogen-FAP complex was used, for example, in live cell STED imaging (Fitzpatrick *et al.*, 2009). Similarly, the Fluorescence-Activating and absorption-Shifting Tag (FAST) binds its fluorogen specifically and reversibly, through which fluorescence can be turned on or off by buffer change (±fluorogen), e.g., using microfluidics. Demonstrated FAST ligands include the green emitting 4-hydroxy-3-methylbenzylidene rhodanine (HMBR, λ_{abs} = 481 nm, λ_{em} = 540 nm, K_D of 1.3×10^{-7} M, fluorogenic ratio of up to 550), as well as yellow and red emitting ligands (Li *et al.*, 2017a; Plamont *et al.*, 2016). A possible FRET donor is 4-hydroxy-3,5-dimethoxybenzylidene rhodanine having λ_{abs} = 518 nm, λ_{em} = 600 nm, K_D of 9.7×10^{-7} M, and fluorogenic ratio = 220. While this is promising for DyeCycling, questions remain about its photostability (Kompa *et al.*, 2023). Also, the relatively big size of the FAST protein tag (14 kDa) and the limitation to amino- or carboxy-terminal labelling positions are not ideal for DyeCycling.

Alternatively, fluorogenic aptamers – here specifically RNA aptamers – bind and increase the fluorescence of their ligand. A large variety of fluorogenic RNA aptamers exist, with emission across the visible range and applications ranging from RNA sensors and transcriptional reporter arrays to super-resolution imaging of RNA (Lu *et al.*, 2023). These aptamer systems function through varied fluorogenic mechanisms: intramolecular charge transfer, contact quenching, or spirocyclization. Interestingly, in some aptamers, the fluorophore molecule binds reversibly and thus can be replaced. For example, the RhoBAST (Rhodamine Binding Aptamer for Super-resolution Imaging Techniques) aptamer has the fluorophore-quencher pair of tetramethylrhodamine (TMR) and dinitroaniline (DN) as the fluorogenic ligand. TMR binding to the aptamer stops contact quenching by DN, leading to a fluorogenic ratio of 26 (Figure 4C). The K_D of $1.5 \pm 0.1 \times 10^{-8}$ M of the RhoBAST system was found suitable for super-resolution imaging

https://doi.org/10.1017/qrd.2024.11 Published online by Cambridge University Press

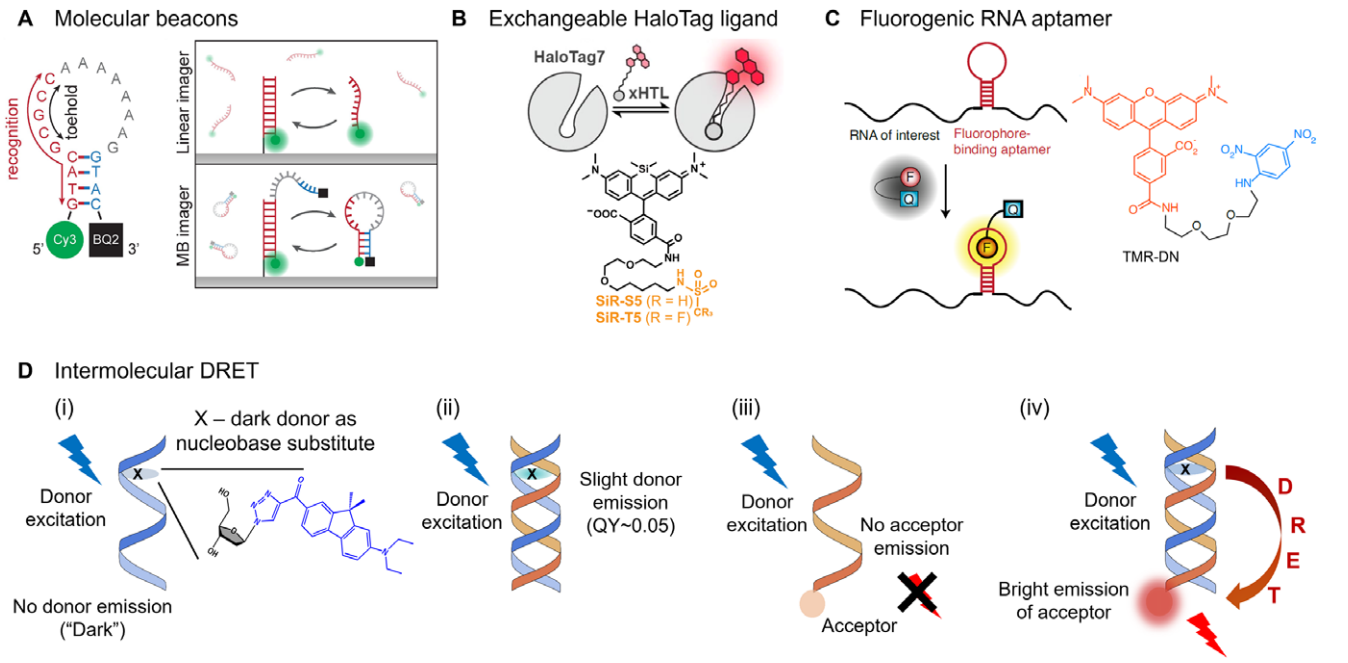

Figure 4. Examples of fluorogenic systems. (A) The molecular beacon (MB) and its application for MB-PAINT. Upon binding to the docking strand, the fluorophore and quencher separate in space, leading to increased fluorophore emission. Image from Kim and Li. 2023. Reprint permission obtained from John Wiley & Sons – Books. (B) Reversible binding of ligands to HaloTag7. The chemical structures of the ligands are shown on the bottom. Image from Kompa et al. (2023). Reprint under OpenAccess with CC BY 4.0. (C) The fluorophore-binding aptamer (Rhodamine Binding Aptamer for Super-resolution Imaging Techniques – RhoBAST) with a contact-quenched fluorophore–quencher (F–Q) conjugate. The RhoBAST RNA sequence and the structure of the F–Q (tetramethylrhodamine (TMR) – dinitroaniline (DN)) are shown. Image from Sunbul et al. (2021). Reprint permission obtained from Springer Nature. (D) Fluorogenicity by energy transfer via DRET. (i) No donor emission is observed in ssDNA (dark). The structure of the dark donor is shown on the right. (ii) Weak donor emission in dsDNA with quantum yield (QY) ~ 0.05. (iii) The acceptor (e.g., Cy5, ATTO 647N) is not excited by the donor excitation wavelength. (iv) Efficient DRET occurs in dsDNA with donor and acceptor on complementary strands.

of a target RNA (Sunbul *et al.*, 2021). While this sounds promising for use in DyeCycling, large aptamers (55 nt for RhoBAST) have similar size limitations to the protein tags above, and the additional negative charge could impair protein activity. However, if there were smaller versions in the future (possibly from peptide nucleic acid, PNA), such minimal fluorogenic aptamers could be a promising option for DyeCycling.

Fluorogenicity via (dark) resonance energy transfer

Intermolecular dark resonant energy transfer (DRET) involves a quenched 'dark' donor and a resonant acceptor with corresponding spectral overlap, and it occurs like FRET via transition dipole coupling of the donor and acceptor. Barnoin et al. (2021) used DialkylaminoFluoreneKetotriazolyl (DFK) as a nucleobase substitute in a DNA oligonucleotide, which served as the DRET donor (Figure 4D). Coupled to ssDNA (QY ~ 0.5%) or duplex DNA (QY ~ 5.5%), little DFK emission is observed, but in the vicinity of a suitable acceptor (e.g., Cy5, ATTO 647N), DRET occurs and the emission of the acceptor is observed. While the low donor QY naturally causes minimal donor background, which is promising for DyeCycling experiments, it also presents a drawback in comparison to FRET, where the mutual anticorrelation of donor and acceptor signals serves as a convenient internal control for data quality. DRET lacks this complementarity, as DRET-sensitised acceptor fluorescence is the only readout. This means, for the DyeCycling experiment, that low-DRET resulting from bona fide biomolecular conformations must be distinguishable from the unbound-acceptor or unbound-donor baseline to prevent their confusion and misinterpretation. This can likely be solved by choosing sufficiently close fluorophore positions, resulting in medium to high DRET. On the other hand, the high Stokes shift of DFK (~200 nm) allows one to select an acceptor causing minimal emission upon donor excitation. Also, given its apparent fluorogenic ratio of ~40 and the ability to tune the DNA binding kinetics, DRET appears as an interesting option for DyeCycling.

Discussion of fluorogenic strategies for DyeCycling

Fluorogenic probes for DyeCycling need to fulfil several requirements, as summarized in Box 1. Several of the techniques discussed in the previous sections fall short of reversibility, such as tetrazine-mediated irreversible IEDDA reactions. For protein tag-derived fluorogenic systems, reversible options exist (e.g., reversible HaloTag ligands (Kompa *et al.*, 2023), FAST protein (Plamont *et al.*, 2016)) but they are limited to end-labelling positions, and their large size (>14 kDa) makes them impractical and insensitive for nanometer-distance changes of biomolecular systems. Similarly, aggregation-caused quenching and aggregation-induced emission are impractical for single-molecule FRET as they involve multiple molecules of the same fluorophore in close proximity.

More promising fluorogenic strategies for DyeCycling are compared in Table 1. They include simple fluorophore-quencher pairs, such as DNA-based molecular beacons with quenching efficiency up to 98% (Marras *et al.*, 2002). Mutually compatible fluorophore-quencher pairs can be selected for use as donor and acceptor, each with individual specificity for a docking strand attached to the biomolecule of interest. Care must be taken to ensure appropriate kinetics, as intra-molecular interactions may reduce the binding rate, which was previously improved by smart

https://doi.org/10.1017/qrd.2024.11 Published online by Cambridge University Press

Table 1. Comparing the potential of fluorogenic systems for DyeCycling: green: suitable, red: not optimal; D: donor, A: acceptor; Michael: Michael reaction of cysteine and maleimide; uaa: unnatural amino acid labelling. † Estimates of the contour length between fluorophore and biomolecule are specified.

Fluorogenic system	Size	Linker length†	Fluorogenic ratio	Dissociation constant (K_D)	k_{off} (s^{-1})	Site-specific bio-conjugation with proteins	References
Fluorophore-quencher pair	D: 15 nt A: 11 nt	~1 nm	D: 16 A: 4	D: 5.5E–8 M A: 4.4E–9 M	D: 0.05 A: 0.07	Variable, e.g., Michael, uaa	Kümmerlin *et al.* (2023)
Molecular Beacons (MBs)	Tot. MB: 21 nt; target: 9 nt	~1 nm	~30	5.5E–5 M	1.2	Variable, e.g., Michael, uaa	Kim and Li (2023)
Reversible HaloTag	34 kDa	~4 nm	10	6.7E–8 M	0.4	C-/N-termini	Kompa *et al.* (2023)
FAST Tag	14 kDa	~3.4 nm	550	1.3E–7 M	6.3	C-/N-termini	Plamont *et al.* (2016)
RhoBAST	55 nt	~2 nm	26	1.5E–8 M	0.7	Variable, e.g., Michael, uaa	Sunbul *et al.* (2021)
Intermolecular DRET	11 nt	~1 nm	~40	1.9E–7 M	0.5	Variable, e.g., Michael, uaa	Barnoin *et al.* (2021) S.G. personal communication

sequence engineering (Kim and Li, 2023). The dissociation rate, on the other hand, scales inversely with the duplex length, which allows one to tune it, e.g., by mismatch insertion (Chung *et al.*, 2022). Since quenching by resonant energy transfer can occur up to 10 nm, effective de-quenching would require relatively long duplexes, causing slow dissociation rates. Thus, short-range (1–2 nm) quenching mechanisms, such as contact, collisional, PET, or Dexter electron transfer-based quenching, appear more favourable, as they are compatible with shorter duplexes with suitable binding kinetics. RNA aptamers with reversibly binding fluorogenic ligands could make useful DyeCycling probes with tuneable binding kinetics, in particular, if small versions (possibly based on peptide nucleic acid) could be derived (Sunbul *et al.*, 2021). Intermolecular DRET (Barnoin *et al.*, 2021), although not conventionally fluorogenic, still presents interesting characteristics for DyeCycling: DNA-based tuneable reversibility, water solubility, and high 'apparent' fluorogenicity of the acceptor. Hence, if the SNR of the DRET-sensitized acceptor fluorescence is sufficiently high, DRET appears as an interesting option for DyeCycling. Lastly, we note that if oligo-based cyclers are used to study RNA/DNA-containing systems, care should be taken not to introduce off-target binding.

Outlook

DyeCycling has the potential to offer better informed smFRET revealing biomolecular mechanisms that are currently beyond the accessible time range (e.g., polymerase pausing, co-translational effects, etc.). *Fluorogenic* DyeCycling would bring these benefits to regular glass (or quartz) slides, bypassing the need for nanophotonics for background suppression. The challenge in implementing fluorogenic DyeCycling lies in finding experimental conditions that meet several requirements simultaneously (Box 1). Donor and acceptor binding should be mutually orthogonal, have suitable binding kinetics (ca. 1/s binding rate, 0.1/s dissociation rate), be compatible with FRET (high overlap integral), and have excellent fluorogenic and photophysical properties (high fluorogenic ratio, brightness, and photostability). Given that the requirements of DyeCycling exceed those of typical imaging applications, it is encouraging that several existing fluorogenic systems appear compliant with fluorogenic DyeCycling. Various DNA, RNA, or PNA-based probes offer much design flexibility in terms of structure, binding kinetics, and diverse commercially available functionalization. Classical fluorophore-quencher pairs can be implemented intra-molecularly based on several short-range quenching mechanisms, which are compatible with short oligos offering suitably fast dissociation rates. Additional strategies worth investigating include small versions of fluorogenic aptamers as well as DRET combined with single-colour detection. Such fluorogenic approaches would benefit not only smFRET via DyeCycling, REFRESH-FRET (Kümmerlin *et al.*, 2023) and FRET X (Filius *et al.*, 2021), but also super-resolution microscopy techniques (Chung *et al.*, 2022). Moreover, there is no fundamental reason limiting the development of new small-molecular and fluorogenic DyeCycling probes, which could be an interesting application of reversible covalent binders or host-guest chemistries, for example, in combination with non-canonical amino acids incorporated via genetic code expansion. Such potential future fluorogenic systems, along with the already existing options, make it very likely that fluorogenic DyeCycling can be implemented and become useful as a next-generation smFRET technique in vitro – and potentially even in cells.

Open peer review. To view the open peer review materials for this article, please visit http://doi.org/10.1017/qrd.2024.11.

Acknowledgements. We thank Pablo Rivera-Fuentes, Oliver S. Wenger, Björn Pfund, Alexandria Deliz Liang and Benjamin Vermeer for helpful discussions.

Author contribution. SS conceived the paper and SG wrote the first draft. Both discussed and edited the paper.

Financial support. This work was supported by the Swiss National Science Foundation as part of the NCCR Molecular Systems Engineering (51NF40–205608) and by the University of Basel.

Competing interest declaration. The authors declare no conflict of interest.

References

Abravaya K, Huff J, Marshall R, Merchant B, Mullen C, Scheider G and Robinson J (2003) Molecular beacons as diagnostic tools: Technology and applications. *Clinical Chemistry and Laboratory Medicine*, **41**(4), 468–474.

Aitken CE, Marshall RA and Puglisi JD (2008) An oxygen scavenging system for improvement of dye stability in single-molecule fluorescence experiments. *Biophysical Journal*, **94**(5), 1826–1835.

Altman RB, Terry DS, Zhou Z, Zheng Q, Geggier P, Kolster RA, Zhao Y, Javitch JA, Warren JD and Blanchard SC (2012) Cyanine fluorophore derivatives with enhanced photostability. *Nature Methods*, **9**(1), 68–71.

Banala S, Maurel D, Manley S and Johnsson K (2012) A caged, localizable rhodamine derivative for superresolution microscopy. *ACS Chemical Biology*, **7**(2), 289–293.

Barnoin G, Shaya J, Richert L, Le H-N, Vincent S, Guérineau V, Mély Y, Michel BY and Burger A (2021) Intermolecular dark resonance energy transfer (DRET): Upgrading fluorogenic DNA sensing. *Nucleic Acids Research*, **49**(12), 1–11.

Beliu G, Kurz AJ, Kuhlemann AC, Behringer-Pliess L, Meub M, Wolf N, Seibel J, Shi ZD, Schnermann M, Grimm JB, Lavis LD, Doose S and Sauer M (2019) Bioorthogonal labeling with tetrazine-dyes for super-resolution microscopy. *Communications Biology*, **2**(1), 261.

Benesch RE and Benesch R (1953) Enzymatic removal of oxygen for polarography and related methods. *Science*, **118**(3068), 447–448.

Brocchieri L and Karlin S (2005) Protein length in eukaryotic and prokaryotic proteomes. *Nucleic Acids Research*, **33**(10), 3390–3400.

Chung KKH, Zhang Z, Kidd P, Zhang Y, Williams ND, Rollins B, Yang Y, Lin C, Baddeley D and Bewersdorf J (2022) Fluorogenic DNA-PAINT for faster, low-background super-resolution imaging. *Nature Methods*, **19**(5), 554–559.

Crisalli P and Kool ET (2011) Multi-path quenchers: Efficient quenching of common fluorophores. *Bioconjugate Chemistry*, **22**(11), 2345–2354.

Crouch GM, Han D and Bohn PW (2018) Zero-mode waveguide nanophotonic structures for single molecule characterization. *Journal of Physics D: Applied Physics*, **51**, 193001.

Deng Y, Shen T, Yu X, Li J, Zou P, Gong Q, Zheng Y, Sun H, Liu X and Wu H (2024) Tetrazine-isonitrile bioorthogonal fluorogenic reactions enable multiplex labeling and wash-free bioimaging of live cells. *Angewandte Chemie International Edition*, **63**(10), e202319853.

Doose S, Neuweiler H and Sauer M (2009) Fluorescence quenching by photoinduced electron transfer: A reporter for conformational dynamics of macromolecules. *ChemPhysChem*, **10**(9–10), 1389–1398.

English BP, Min W, Van Oijen AM, Kang TL, Luo G, Sun H, Cherayil BJ, Kou SC and Xie XS (2006) Ever-fluctuating single enzyme molecules: Michaelis-Menten equation revisited. *Nature Chemical Biology*, **2**(2), 87–94.

Filius M, Kim SH, Severins I and Joo C (2021) High-resolution single-molecule FRET via DNA eXchange (FRET X). *Nano Letters*, **21**(7), 3295–3301.

Fitzpatrick JAJ, Yan Q, Sieber JJ, Dyba M, Schwarz U, Szent-Gyorgyi C, Woolford CA, Berget PB, Waggoner AS and Bruchez MP (2009) STED nanoscopy in living cells using fluorogen activating proteins. *Bioconjugate Chemistry*, **20**(10), 1843–1847.

Fölling J, Belov V, Kunetsky R, Medda R, Schönle A, Egner A, Eggeling C, Bossi M and Hell SW (2007) Photochromic rhodamines provide nanoscopy with optical sectioning. *Angewandte Chemie International Edition*, **46**(33), 6266–6270.

Goldberg JM, Batjargal S, Chen BS and Petersson EJ (2013) Thioamide quenching of fluorescent probes through photoinduced electron transfer: Mechanistic studies and applications. *Journal of the American Chemical Society*, **135**(49), 18651–18658.

Ha T, Fei J, Schmid S, Lee NK, Gonzalez RL, Paul S and Yeou S (2024) Fluorescence resonance energy transfer at the single-molecule level. *Nature Reviews Methods Primers*, **4**(1), 21.

Hanczyc P, Rajchel-Mieldzioć P, Feng B and Fita P (2021) Identification of thioflavin T binding modes to DNA: A structure-specific molecular probe for lasing applications. *Journal of Physical Chemistry Letters*, **12**(22), 5436–5442.

Hellenkamp B, Schmid S, Doroshenko O, Opanasyuk O, Kühnemuth R, Rezaei Adariani S, Ambrose B, Aznauryan M, Barth A, Birkedal V, Bowen ME, Chen H, Cordes T, Eilert T, Fijen C, Gebhardt C, Götz M, … Hugel T (2018) Precision and accuracy of single-molecule FRET measurements—A multi-laboratory benchmark study. *Nature Methods*, **15**(9), 669–676.

Hyeon C, Lee J, Yoon J, Hohng S and Thirumalai D (2012) Hidden complexity in the isomerization dynamics of Holliday junctions. *Nature Chemistry*, **4**(11), 907–914.

Isselstein M, Zhang L, Glembockyte V, Brix O, Cosa G, Tinnefeld P and Cordes T (2020) Self-healing dyes-keeping the promise? *Journal of Physical Chemistry Letters*, **11**(11), 4462–4480.

Janissen R, Eslami-Mossallam B, Artsimovitch I, Depken M and Dekker NH (2022) High-throughput single-molecule experiments reveal heterogeneity, state switching, and three interconnected pause states in transcription. *Cell Reports*, **39**(4), 110749.

Jungmann R, Steinhauer C, Scheible M, Kuzyk A, Tinnefeld P and Simmel FC (2010) Single-molecule kinetics and super-resolution microscopy by fluorescence imaging of transient binding on DNA origami. *Nano Letters*, **10**(11), 4756–4761.

Kim SH and Li ITS (2023) Super-resolution tension PAINT imaging with a molecular Beacon. *Angewandte Chemie International Edition*, **62**(7), e202217028.

Klymchenko AS (2017) Solvatochromic and fluorogenic dyes as environment-sensitive probes: Design and biological applications. *Accounts of Chemical Research*, **50**(2), 366–375.

Kompa J, Bruins J, Glogger M, Wilhelm J, Frei MS, Tarnawski M, D'Este E, Heilemann M, Hiblot J and Johnsson K (2023) Exchangeable HaloTag ligands for super-resolution fluorescence microscopy. *Journal of the American Chemical Society*, **145**(5), 3075–3083.

Kozma E and Kele P (2019) Fluorogenic probes for super-resolution microscopy. *Organic and Biomolecular Chemistry*, **17**(2), 215–233.

Kümmerlin M, Mazumder A and Kapanidis AN (2023) Bleaching-resistant, near-continuous single-molecule fluorescence and FRET based on fluorogenic and transient DNA binding. *ChemPhysChem*, **24**(12), e202300175.

Le Reste L, Hohlbein J, Gryte K and Kapanidis AN (2012) Characterization of dark quencher chromophores as nonfluorescent acceptors for single-molecule FRET. *Biophysical Journal*, **102**(11), 2658–2668.

Lee MK, Rai P, Williams J, Twieg RJ and Moerner WE (2014) Small-molecule labeling of live cell surfaces for three-dimensional super-resolution microscopy. *Journal of the American Chemical Society*, **136**(40), 14003–14006.

Lerner E, Barth A, Hendrix J, Ambrose B, Birkedal V, Blanchard SC, Börner R, Chung HS, Cordes T, Craggs TD, Deniz AA, Diao J, Fei J, Gonzalez RL, Gopich I V., Ha T, Hanke CA, … Boudker O (2021) FRET-based dynamic structural biology: Challenges, perspectives and an appeal for open-science practices. *eLife*, **10**, e60416.

Levene MJ, Korlach J, Turner SW, Foquet M, Craighead HG and Webb WW (2002) Zero-mode waveguides for single-molecule analysis at high concentrations, *Science*, **299**(5607), 682–686.

Li C, Plamont MA, Sladitschek HL, Rodrigues V, Aujard I, Neveu P, Le Saux T, Jullien L and Gautier A (2017a) Dynamic multicolor protein labeling in living cells. *Chemical Science*, **8**(8), 5598–5605.

Li C, Tebo AG and Gautier A (2017b) Fluorogenic labeling strategies for biological imaging. *International Journal of Molecular Sciences*, **18**(7), 1473.

Liu Y, Fares M, Dunham NP, Gao Z, Miao K, Jiang X, Bollinger SS, Boal AK and Zhang X (2017) AgHalo: A facile fluorogenic sensor to detect drug-induced proteome stress. *Angewandte Chemie*, **129**(30), 8798–8802.

Loredo A, Tang J, Wang L, Wu KL, Peng Z and Xiao H (2020) Tetrazine as a general phototrigger to turn on fluorophores. *Chemical Science*, **11**(17), 4410–4415.

Lu X, Kong KYS and Unrau PJ (2023) Harmonizing the growing fluorogenic RNA aptamer toolbox for RNA detection and imaging. *Chemical Society Reviews*, **52**, 4071–4098.

Marras SAE, Kramer FR and Tyagi S (2002) Efficiencies of Fuorescence resonance energy transfer and contact-mediated quenching in oligonucleotide probes. *Nucleic Acids Research*, **30**(21), e122.

Martin A and Rivera-Fuentes P (2024) A general strategy to develop fluorogenic polymethine dyes for bioimaging. *Nature Chemistry*, **16**(1), 28–35.

Mei J, Leung NLC, Kwok RTK, Lam JWY and Tang BZ (2015) Aggregation-induced emission: Together we Shine, united we soar! *Chemical Reviews*, **115**(21), 11718–11940.

Nova IC, Craig JM, Mazumder A, Laszlo AH, Derrington IM, Noakes MT, Brinkerhoff H, Yang S, Vahedian-Movahed H, Li L, Zhang Y, Bowman JL, Huang JR, Mount JW, Ebright RH and Gundlach JH (2024) Nanopore tweezers show fractional-nucleotide translocation in sequence-dependent pausing by RNA polymerase. *Proceedings of the National Academy of Sciences of the United States of America*, **121**(29), e2321017121.

https://doi.org/10.1017/qrd.2024.11 Published online by Cambridge University Press

van Oijen AM, **Blainey PC**, **Crampton DJ**, **Richardson CC**, **Ellenberger T and Xie XS** (2003) Single-molecule kinetics of λ exonuclease reveal base dependence and dynamic disorder. *Science*, **301**, 1235–1238.

Pati AK, **Bakouri O El**, **Jockusch S**, **Zhou Z**, **Altman RB**, **Fitzgerald. GA**, **Asher WB**, **Terry DS**, **Borgia A**, **Holsey MD**, **Batchelder JE.**, **Abeywickrama C**, **Huddle B**, **Rufa D**, **Javitch JA**, **Ottosson henrik and Blanchard SC** (2020) Tuning the Baird aromatic triplet-state energy of cyclooctatetraene to maximize the self-healing mechanism in organic fluorophores. *Proceedings of the National Academy of Sciences of the United States of America*, **117**(39), 24305–24315.

Pinto-Pacheco B, **Carbery WP**, **Khan S**, **Turner DB and Buccella D** (2020) Fluorescence quenching effects of tetrazines and their Diels–Alder products: Mechanistic insight toward fluorogenic efficiency. *Angewandte Chemie International Edition*, **59**(49), 22140–22149.

Plamont MA, **Billon-Denis E**, **Maurin S**, **Gauron C**, **Pimenta FM**, **Specht CG**, **Shi J**, **Quérard J**, **Pan B**, **Rossignol J**, **Morellet N**, **Volovitch M**, **Lescop E**, **Chen Y**, **Triller A**, **Vriz S**, **Le Saux T**, **… Gautier A** (2016) Small fluorescence-activating and absorption-shifting tag for tunable protein imaging in vivo. *Proceedings of the National Academy of Sciences of the United States of America*, **113**(3), 497–502.

Rasnik I, **McKinney SA and Ha T** (2006) Nonblinking and long-lasting single-molecule fluorescence imaging. *Nature Methods*, **3**(11), 891–893.

Rosing J and Slater EC (1971) The value of ΔG° for the hydrolysis of ATP. *Biochemica et Biophysica Acta*, **267**, 275–290.

Roy R, **Hohng S and Ha T** (2008) A practical guide to single-molecule FRET. *Nature Methods*, **5**(6), 507–516.

Sharonov A and Hochstrasser RM (2006) Wide-field subdiffraction imaging by accumulated binding of diffusing probes. *Proceedings of the National Academy of Sciences of the United States of America*, **103**(50), 18911–18916.

Si D, **Li Q**, **Bao Y**, **Zhang J and Wang L** (2023) Fluorogenic and cell-permeable rhodamine dyes for high-contrast live-cell protein labeling in bioimaging and biosensing. *Angewandte Chemie International Edition*, **62**(45), e202307641.

Sunbul M and Jäschke A (2013) Contact-mediated quenching for RNA imaging in bacteria with a fluorophore-binding aptamer. *Angewandte Chemie International Edition*, **52**(50), 13401–13404.

Sunbul M, **Lackner J**, **Martin A**, **Englert D**, **Hacene B**, **Grün F**, **Nienhaus K**, **Nienhaus GU and Jäschke A** (2021) Super-resolution RNA imaging using a rhodamine-binding aptamer with fast exchange kinetics. *Nature Biotechnology*, **39**(6), 686–690.

Sustarsic M and Kapanidis AN (2015) Taking the ruler to the jungle: Single-molecule FRET for understanding biomolecular structure and dynamics in live cells. *Current Opinion in Structural Biology*, **34**, 52–59.

Swoboda M, **Henig J**, **Cheng HM**, **Brugger D**, **Haltrich D**, **Plumeré N and Schlierf M** (2012) Enzymatic oxygen scavenging for photostability without ph drop in single-molecule experiments. *ACS Nano*, **6**(7), 6364–6369.

Tsai A, **Puglisi JD and Uemura S** (2016) Probing the translation dynamics of ribosomes using zero-mode waveguides. *Progress in Molecular Biology and Translational Science*, **139**, 1–43.

Tyagi S and Kramer FR (1996) Molecular beacons: Probes that fluoresce upon hybridization, *Nature Biotechnology*, **14**, 303–308.

Vermeer B and Schmid S (2022) Can DyeCycling break the photobleaching limit in single-molecule FRET? *Nano Research*, **15**(11), 9818–9830.

Vogelsang J, **Kasper R**, **Steinhauer C**, **Person B**, **Heilemann M**, **Sauer M and Tinnefeld P** (2008) A reducing and oxidizing system minimizes photobleaching and blinking of fluorescent dyes. *Angewandte Chemie International Edition*, **47**(29), 5465–5469.

Wang C and Yang CJ (2013) Application of molecular Beacons in real-time PCR. In *Molecular Beacons*. Berlin Heidelberg: Springer-Verlag, pp.45–59.

Werther P, **Yserentant K**, **Braun F**, **Grußmayer K**, **Navikas V**, **Yu M**, **Zhang Z**, **Ziegler MJ**, **Mayer C**, **Gralak AJ**, **Busch M**, **Chi W**, **Rominger F**, **Radenovic A**, **Liu X**, **Lemke EA**, **Buckup T**, **… Wombacher R** (2021) Bio-orthogonal red and far-red fluorogenic probes for wash-free live-cell and super-resolution microscopy. *ACS Central Science*, **7**(9), 1561–1571.

Yang S, **Klughammer N**, **Barth A**, **Tanenbaum ME and Dekker C** (2023) Zero-mode waveguide nanowells for single-molecule detection in living cells. *ACS Nano*, **17**(20), 20179–20193.

Zhao E and Chen S (2021) Materials with aggregation-induced emission characteristics for applications in diagnosis, theragnosis, disease mechanism study and personalized medicine. *Materials Chemistry Frontiers*, **5**, 3322–3343.

Zhao E, **Chen Y**, **Chen S**, **Deng H**, **Gui C**, **Leung CWT**, **Hong Y**, **Lam JWY and Tang BZ** (2015) A luminogen with aggregation-induced emission characteristics for wash-free bacterial imaging, high-throughput antibiotics screening and bacterial susceptibility evaluation. *Advanced Materials*, **27**(33), 4931–4937.

Zheng Q, **Juette MF**, **Jockusch S**, **Wasserman MR**, **Zhou Z**, **Altman RB and Blanchard SC** (2014) Ultra-stable organic fluorophores for single-molecule research. *Chemical Society Reviews*, **43**(4), 1044–1056.

Zheng Q and Lavis LD (2017) Development of photostable fluorophores for molecular imaging. *Current Opinion in Chemical Biology*, **39**, 32–38.

https://doi.org/10.1017/qrd.2024.11 Published online by Cambridge University Press